

# Synthesis, spectral, solvent dependent linear and nonlinear optical characteristics of (E)-N-(3-(3-(4(dimethylamino)phenyl)acryloyl)phenyl)quinolone-2-carboxamide

SUDHA N (✉ [sudhaucet@gmail.com](mailto:sudhaucet@gmail.com))

University College of Engineering Tindivanam, Anna University Chennai <https://orcid.org/0000-0002-8058-6763>

R Surendran

University College of Engineering Tindivanam, Anna University Chennai

S Jeyaram

Surya Group of Institutions

---

## Research Article

**Keywords:** Quinolinecarboxamide Chalcone, TNLO, Z-scan, polar solvents, spectral characteristics

**Posted Date:** March 9th, 2022

**DOI:** <https://doi.org/10.21203/rs.3.rs-1401196/v1>

**License:** © ⓘ This work is licensed under a Creative Commons Attribution 4.0 International License.

[Read Full License](#)

---

# Synthesis, spectral, solvent dependent linear and nonlinear optical characteristics of (E)-N-(3-(3-(4(dimethylamino)phenyl)acryloyl)phenyl)quinolone-2-carboxamide

N. Sudha<sup>1,\*</sup>, R. Surendran<sup>2</sup> and S. Jeyaram<sup>3</sup>

<sup>1</sup>Department of Physics, University College of Engineering Tindivanam, Anna University Chennai, Tamilnadu, India.

<sup>2</sup>Department of Physics, University College of Engineering Nagercoil, Anna University Chennai, Tamilnadu, India.

<sup>3</sup>Department of Physics, School of Engineering and Technology, Surya Group of Institutions, Villupuram-605652, Tamilnadu, India.

## Email

sudhaucet@gmail.com

## Abstract

This paper presents the synthesis of novel organic compound (E)-N-(3-(3-(4(dimethylamino)phenyl)acryloyl)phenyl)quinolone-2-carboxamide, also known as Quinolinecarboxamide Chalcone (QCC) using aldol condensation and carboxamide formation method. The organic sample QCC was examined by FT-IR, <sup>1</sup>H NMR, <sup>13</sup>C NMR and mass spectroscopic techniques, respectively. Linear and third-order nonlinear optical (TNLO) properties of QCC dissolved in polar solvents such as DMSO, DMF and Ethanol have also been studied. The order of nonlinear refractive index and nonlinear absorption coefficient of QCC was measured to be  $10^{-11}$  m<sup>2</sup>/W and  $10^{-5}$  m/W. The nonlinear refractive index ( $n_2$ ) of QCC was attributed to negative nonlinearity due to self-defocusing effect, and nonlinear absorption coefficient ( $\beta$ ) indicates the behaviors of saturable absorption (SA) and reverse saturable absorption (RSA). The real and imaginary features of the TNLO susceptibility ( $\chi^{(3)}$ ) of QCC in polar solvents were calculated to be the order of  $10^{-7}$  esu. The spectral characteristics of solvent on TNLO susceptibility of QCC were discussed. The results divulged that the synthesized organic compound is a novel nonlinear optical (NLO) material for applications in photonics and optoelectronics.

**Keywords:** Quinolinecarboxamide Chalcone, TNLO, Z-scan, polar solvents, spectral characteristics.

## Introduction

The extensive use of nonlinear optical (NLO) materials in the field of science and technology, such as optical computing, optical data storage, optical limiting, up conversion lasing, two-photon microscopy and optical switching [1-5], have prompted the researchers to develop novel materials suitable for NLO applications. Variety of materials [6-11] are known to be optically nonlinear and exhibits large TNLO susceptibility under pulsed and continuous wave regime. Among them, organic molecules have always attracted the attention of researchers owing to high molecular polarizability, chemical stability, fast response time and possess large  $\pi$ -conjugated electrons [12-14]. The chemical structure of organic molecules can be fine-tuned to achieve the desired NLO properties. In comparison to inorganic materials, they have high laser damage threshold and a low dielectric constant [15]. The delocalization of electronic charge distribution in organic molecules leads to a high mobility due to overlapping of  $\pi$  orbitals which leads to large NLO properties.

The physical and chemical behavior of organic molecules is strongly related to its molecular structure [8]. Solvent parameters are the significant factors that affect the NLO features of the molecules. Therefore, the influence of solvent on linear and nonlinear characteristics of organic molecules has been the subject of several investigations [16]. The solute-solvent interactions are commonly described in terms of non-specific (van der Waals) and specific (hydrogen bond) interaction [17]. Specific and non-specific interaction between solute and solvent is accountable for modification of molecular geometry, electronic structure, and dipole moment of the solute [18].

Z-scan technique [19] is the sensitive experiment for determining the TNLO properties of the organic compound. Despite the fact that there are a variety of techniques for measuring the nonlinear optical characteristics, Z-scan method have received considerable attention from the scientific community due to simplicity, sensitivity and ability to produce immediate results. Z-scan technique employs the principle of spatial self-phase modulation in which the phase modulation is transferred to amplitude modulation. This paper reports the synthesis, characterization and solvent dependent linear and TNLO features of novel organic compound QCC. The TNLO properties of the organic compound dissolved in various polar solvents such as DMSO, DMF and ethanol was measured by Z-scan method with an operating wavelength of 650 nm.

## Materials and methods

### Synthesis of (E)-1-(3-aminophenyl)-3-(4-(dimethylamino)phenyl)prop-2-en-1-one (3)

3-amino acetophenone (1.0 g, 7.376 mmol) and *p*-N,N-dimethyl benzaldehyde (1.103 g, 7.376 mmol) was dissolved in Ethanol (20 mL). To that solution, sodium hydroxide solution (1,183g, 29.59 mmol, dissolved in 2 mL water) was added and the reaction mixture was stirred for an hour. The resultant precipitate was filtered and washed with a small amount of ethanol. The product was dried in air for 24 h and taken to the next step.

### Synthesis of (E)-N-(3-(3-(4-(dimethylamino)phenyl)acryloyl)phenyl)quinoline-2-carboxamide (QCC)

The quinoline-2-carboxylic acid (0.5 g, 2.89 mmol) was dissolved in acetonitrile (20 mL). To that solution, TBTU (1.113 g, 3.468 mmol) and triethylamine (0.6 mL, 4.335 mmol) was added and the reaction mixture was stirred at room temperature for 30 min. Finally, the intermediate 3 (0.769g, 2.89 mmol) was added and the reaction mixture was stirred for 3 h. The completion of the reaction was monitored by TLC. The reaction mixture was diluted with ethyl acetate and washed with sodium bicarbonate solution, water and brine solution. The organic layer was separated and dried over anhydrous Na<sub>2</sub>SO<sub>4</sub>. The final compound QCC was obtained by evaporating the solvents. The synthetic route and molecular structure of QCC is represented in Figs. 1 and 2.

## Instrumentation

The FT-IR spectrum of QCC is recorded using Thermo Scientific Nicolet iS50 FT-IR Spectrometer. The UV absorption spectra of the organic compound QCC was measured using Labman (LMSP-UV1200) UV-Vis spectrometer. <sup>1</sup>H NMR and <sup>13</sup>C NMR spectra were recorded by Bruker 500 MHz and 125 MHz instruments in DMSO-D<sub>6</sub> for proton and carbon spectra. Chemical shift values are mentioned in δ (ppm) and coupling constants are given in Hz. LCQ Fleet mass spectrometer, Thermo Fisher Instruments Limited, US was used to record mass spectra.

## NMR Spectroscopy

$^1\text{H}$  NMR (500 MHz, DMSO)  $\delta$  11.05 (s, 1H), 8.73 – 8.67 (m, 2H), 8.36- 8.32 (m, 3H), 8.20 (d,  $J = 7.9$  Hz, 1H), 8.03 – 7.95 (m, 2H), 7.84 - 7.81 (m, 1H), 7.78 – 7.77 (m, 3H), 7.73 – 7.63 (m, 2H), 6.82 (d,  $J = 8.9$  Hz, 2H), 3.07 (s, 6H).  $^{13}\text{C}$  NMR (125 MHz, DMSO- $\text{D}_6$ )  $\delta$  188.93, 163.51, 152.56, 150.39, 146.42, 145.89, 139.51, 139.25, 138.79, 131.32, 131.25, 129.87, 129.65, 129.51, 128.97, 128.70, 124.65, 124.39, 122.43, 120.59, 119.32, 116.54, 112.27, 40.22. ESI-Mass: calculated 421.18 m/z, found 422.88 (M+1) $^+$ . FT-IR (KBr Disc)  $\text{cm}^{-1}$ : 3324, 3065, 2901, 2819, 1685, 1648, 1564, 1524, 1184, 1162, 1122, 800, 764.

### Z-scan method

Z-scan method is a potential technique for measuring the TNLO properties of QCC [19]. A diode laser operating at 650 nm wavelength with power of 5 mW was used. Convex lens of 5 cm focal length was placed between light source and sample, in order to effectively focus the beam on to the sample. Two methods namely, closed aperture (CA) and open aperture (OA) were used to determine the nonlinear refraction and absorption of the sample. In CA mode, the aperture with suitable opening size was used, while in OA case, the convex lens was used to collect the transmittance of the sample. A cuvette of thickness 1 mm was placed on the micrometer translational stage and moves the sample between  $-20$  mm and  $+20$  mm positions. The detector was used to measure the transmittance and placed at far-field position. The thin sample condition is validated because the sample length is less than measured Rayleigh length. Fig. 3 displays the Z-scan experimental technique.

## Results and discussion

### Synthesis

The intermediate 3 was synthesized by regular aldol condensation reaction. The reaction of 3-aminoacetophenone with *p*-N,N-dimethyl benzaldehyde in the presence of sodium hydroxide yielded intermediate 3. The QCC was synthesized by regular carboxamide formation. The TBTU was used as a coupling agent, the reaction of quinoline-2-carboxylic acid with intermediate 3 yielded QCC.

### NMR spectroscopy study

The total number of protons in QCC is 23, which is confirmed by  $^1\text{H}$  NMR spectra. The appearance of singlet at 3.06 ppm for 6 protons indicates the presence of N,N dimethyl unit. The signals around 6.82 ppm and 7.78-7.77 ppm appeared for phenylene protons (H26 &

H28, H25 & H29). The carboxamide NH proton appeared as a singlet at 11.05 ppm and the alkene CH appeared in the region of 8.03-7.95 ppm and 7.73-7.63 ppm, respectively. One of the phenylene H19 proton appeared in the region of 7.73-7.63 ppm. The quinoline protons appeared as multiplet at 8.36-8.32, 8.20, 8.03-7.95 and 7.73-7.63 ppm, correspondingly. Similarly, the  $^{13}\text{C}$  NMR also confirms the product formation. The total number of carbon in QCC is 27 and the possible  $^{13}\text{C}$  signals for QCC are 24. The  $^{13}\text{C}$  NMR spectra clearly showed the 24 carbon signals. The carbonyl carbon appeared at 188.93 ppm and the carboxamide carbon appeared at 163.51 ppm, respectively. The C27 quarternary carbon adjacent to N,N-dimethyl unit and the C14 quarternary carbon adjacent to carboxamide nitrogen appeared at 156.52 and 150.39 ppm. The quinoline quarternary carbons C2 and C10 appeared at 146.42 and 145.89 ppm. Fig. 4 depicts the selected  $^1\text{H}$  NMR  $^{13}\text{C}$  NMR chemical shifts of QCC. The  $^1\text{H}$  NMR and  $^{13}\text{C}$  NMR spectrum of QCC are represented in Figs. 5 and 6.

### ESI-Mass spectrum

The Mass spectrum of QCC is shown in Fig. 7. The organic compound QCC is additionally confirmed by ESI-Mass spectrum. The molecular weight of QCC is 421.18 m/z. The positive mode signal appeared as a parent ion peak at 422.88 m/z which is additional evidence for the QCC formation.

### FT-IR study

The FT-IR spectrum of QCC is depicted in Fig. 8 and the vibrational frequencies are denoted by using standard IR table [8]. The weak band at  $3324\text{ cm}^{-1}$  is associated with stretching of N-H group. The stretching frequencies at  $3065$  and  $2901\text{ cm}^{-1}$  appeared for aromatic C-H stretching and the frequency appeared at  $2819\text{ cm}^{-1}$  indicates the presence of aliphatic C-H stretching which belongs to  $\text{CH}_3$  unit of QCC. A strong intense peak at  $1685\text{ cm}^{-1}$  is the result of stretching of C=O group which is present as a  $\alpha$ ,  $\beta$ -unsaturated ketone. The intense vibrational frequencies at  $1648\text{ cm}^{-1}$  are due to carboxamide carbonyl group which is responsible for intersystem crossing transfer (ICT) between donor and acceptor electrons [8]. A sharp intense peak at  $1563\text{ cm}^{-1}$  and  $1524\text{ cm}^{-1}$  is owing to C=C stretching frequencies. The weak band at  $1184$ ,  $1162$  and  $1122\text{ cm}^{-1}$  confirms the presence of C-N stretching group, three different C-N stretching units are present in QCC. Furthermore, the weak bands at  $800\text{ cm}^{-1}$  and  $764\text{ cm}^{-1}$  are related to bending of C-H group.

### **Linear absorption study**

The linear absorption coefficient of QCC in different polar solvents was studied by UV-Visible spectrophotometer between 200 nm and 600 nm. The solvent polarity has a significant impact on the linear absorption coefficient of QCC. The UV-visible absorption spectra of QCC dissolved in different polar solvents such as DMSO, DMF and ethanol is depicted in Fig.9. The coefficient of linear absorption of QCC dissolved in ethanol and DMF is considerably high compare to the sample dissolved in DMSO. The sample dissolved in high polar solvent such as DMSO exhibits small linear absorption coefficient resulting in large value of nonlinear refraction and TNLO susceptibility. The UV-visible absorption spectrum covers the entire visible region and observed that the shift towards red region by increasing the solvent polarity which is the result of positive solvatochromism.

### **Solvent dependent TNLO study**

TNLO characteristics of QCC are measured from OA and CA methods, respectively. The  $\beta$  of the sample is measured from OA technique which is proportional to imaginary component of TNLO susceptibility. The  $n_2$  of organic compound is obtained from CA method which is related to real component of TNLO susceptibility. Fig.10 displays the result of OA Z-scan curve of QCC dissolved in DMSO, DMF and ethanol at 0.01 mM concentration. The OA graph shows both positive and negative nonlinear coefficient of absorption is due to SA and RSA characteristics. The OA Z-scan graph of QCC dissolved in ethanol exhibits SA, while the sample exhibits RSA signature in DMSO and DMF. Both SA and RSA are the characteristic features of the materials that result from an increase or decrease in light transmittance at the focus ( $Z=0$ ). The intensity at the focus is maximum and forms a fine peak is the result of SA. SA ascends from high input intensities, which causes a considerable increase in photon absorption before relaxing to the ground state. On the other hand, the sample dissolved in DMSO and DMF exhibits the character of RSA, owing to strong interaction of light intensity with the sample at the focus and consequently the transmittance decreases at the focus. The absorption cross-section of excited state is greater than ground state which is the result of RSA. Furthermore, RSA of the sample elucidates by the five-level model and the detailed explanation is presented in our recently work [18]. The normalized transmittance from OA Z-scan technique is given by,

$$T(z, s = 1) = \sum_{m=0}^{\infty} \frac{[-q_o(z)]^m}{[m+1]^{\frac{3}{2}}}, \text{ for } |q_o(0)| < 1 \quad (1)$$

where

$$q_o = \frac{\beta I_o L_{eff}}{\left(1 + Z^2/Z_0^2\right)} \quad (2)$$

where  $L_{eff}$  and  $Z_0$  are the sample effective and diffraction length, respectively. The absorption coefficient  $\beta$  of QCC in polar solvents is given by,

$$\beta = \frac{2\sqrt{2}\Delta T}{I_o L_{eff}} \left(\frac{cm}{W}\right) \quad (3)$$

The nonlinear refraction of QCC dissolved in DMSO, DMF and ethanol is determined from CA Z-scan method. The measurement from CA method includes the contribution of nonlinear absorption (NLA). The pure nonlinear refraction is obtained by dividing CA data from the corresponding OA data. The pure nonlinear refraction curve of QCC in different polar solvents is shown in Fig.11. The transmittance curve exhibits a pre focal peak followed by post focal valley is the signature of self-defocusing or negative nonlinear refraction. The self-defocusing effect in organic sample is the outcome of thermal nonlinearity which ascends from continuous absorption of light source at 650 nm wavelength. The transmittance of the sample in different polar solvents is given by,

$$T(z) = 1 - \Delta\phi_o \frac{4X}{(X^2 + 1)(X^2 + 9)} \quad (4)$$

where  $X=Z/Z_0$ . The  $n_2$  is determined by using the relation

$$n_2 = \frac{\Delta\phi_o \lambda}{2\pi I_o L_{eff}} \left(\frac{m^2}{W}\right) \quad (5)$$

where  $\Delta\phi_o$ ,  $\lambda$  and  $I_o$  are on-axis phase shift, wavelength and intensity of the light beam.

The value of  $n_2$  of QCC in polar solvents is presented in Table 1. It is obvious that the nonlinear index of refraction of the sample in DMSO is higher than that of other polar solvents.

The real and imaginary factors of TNLO susceptibility is given by,

$$Re[\chi^{(3)}](esu) = \frac{\epsilon_0 c^2 n_0^2}{10^4 \pi} n_2 \left(\frac{m^2}{W}\right) \quad (6)$$

$$Im[\chi^{(3)}](esu) = \frac{\varepsilon_0 c^2 n_0^2 \lambda}{10^2 4\pi^2} \beta \left( \frac{m}{W} \right) \quad (7)$$

where  $\varepsilon_0$  = vacuum permittivity and  $c$  = velocity of light in vacuum. The TNLO susceptibility was determined by,

$$\chi^{(3)} = \sqrt{(Re(\chi^3))^2 + (Im(\chi^3))^2} (esu) \quad (8)$$

The measured values of TNLO parameters of QCC in polar solvents are presented in Table 1. It is observed from Table 1 that, the TNLO susceptibility of QCC in DMSO exhibits large value compared with other polar solvents such as DMF and ethanol. Further, the synthesized organic compound exhibits large TNLO susceptibility than some recently reported materials [20-23].

Solvent polarity parameters are the major factor affecting the TNLO properties of the sample. The sample was influenced by various spectral features of solvents such as hydrogen bond donor, hydrogen bond acceptor, solvent polarizability and the dipole moment. The change in sign from negative to positive (SA to RSA) in Fig. 10 is the result of solvent polarizability of the solvent. The organic compound QCC is dissolved in low polar solvents such as ethanol exhibits SA behavior, whereas in high polar solvents such as DMSO and DMF exhibits RSA. The value of  $n_2$  and TNLO susceptibility of QCC is increased by increasing solvent polarizability of the solvent. Furthermore, the solvent hydrogen bond donor and acceptor also influence the sample characteristics. The dipole moment plays an important role in the present work. The dipole moment of DMSO, DMF and ethanol is 4.10, 3.86 and 1.69, respectively. The organic compound exhibits large nonlinearity by dissolving DMSO which has high dipole moment. Fig. 12 (a) & (b) depicts the variation of TNLO susceptibility of QCC as a function of solvent polarizability and dipole moment.

## Conclusion

The organic compound QCC was synthesized and examined by FT-IR,  $^1\text{H}$  NMR,  $^{13}\text{C}$  NMR and mass spectroscopic techniques. The polar solvent effect on linear and nonlinear characteristics of the organic compound was studied. The nonlinear refractive index of QCC in polar solvents was ascribed to negative nonlinearity or self-defocusing due to thermal effect. The nonlinear coefficient of absorption of the sample was attributed to both SA and RSA behaviors. The order of TNLO susceptibility of the organic compound was found to be  $10^{-7}$  esu and exhibits large nonlinearity at high polar solvent (DMSO). The nonlinear parameters were increased with increase in solvent polarity. The obtained results suggest that the synthesized organic compound QCC is a novel candidate for NLO applications.

**Funding:** No funding agencies

**Conflict of Interest:** The authors declare that they have no conflict of interest.

**Ethics approval:** The submitted work should be original and should not have been published elsewhere in any form or language.

**Consent to participate:** Research involving human participants

**Consent for publication:** Yes granted

**Data availability:** The datasets generated during the current study is available from the corresponding author.

**Code availability:** The code using the current study is available from the corresponding author.

**Author Contribution:** Conceptualization–NS and SJ; Methodology–RS and SJ; Validation–NS and RS; Writing-review and editing–NS and RS; Supervision–NS.

## References

1. Sreenath MC, Hubert Joe I, Rastogi VK (2018) Third-order optical nonlinearities of 1,-diaminoanthraquinone for optical limiting applications. *Opt Laser Technol* 108: 218–234. <https://doi.org/10.1016/j.optlastec.2018.06.056>.
2. You JW, Bongu SR, Bao A, Panoiu NC (2019) Nonlinear optical properties and applications of 2D materials: theoretical and experimental aspects. *J Nanophotonics* 8: 63–97. <https://doi.org/10.1515/nanoph-2018-0106>.
3. Sangeetha K, Thamotharan S (2018) Thermally induced self-phase modulation and optical limiting applications of L-arginine hydrochloride (LAHCL) solutions. *Optik* 164: 519–526. <https://doi.org/10.1016/j.ijleo.2018.03.029>.
4. Jeyaram S, Hemalatha S, Geethakrishnan T (2020) Nonlinear refraction, absorption and optical limiting properties of disperse blue 14 dye. *Chem Phys Lett* 739: 137037. <https://doi.org/10.1016/j.cplett.2019.137037>.
5. Jeyaram S, Geethakrishnan T (2019) Linear and nonlinear optical properties of chlorophyll-*a* extracted from *Andrographis paniculata* leaves. *Opt Laser Technol* 116: 31–36. <https://doi.org/10.1016/j.optlastec.2019.03.013>.
6. Jeyaram S, Geethakrishnan T (2020) Spectral and third-order nonlinear optical characteristics of natural pigments extracted from coriandrum sativum. *Opt Mater* 107: 110148. <https://doi.org/10.1016/j.optmat.2020.110148>.
7. Zongo S, Sanusi K, Britton J, Mthunzi P, Nyokong T, Maaza M, Sahraoui B (2015) Nonlinear optical properties of natural laccaic dye studied using Z-scan technique. *Opt Mater* 46: 270–275. <https://doi.org/10.1016/j.optmat.2015.04.031>.
8. Jeyaram S (2021) Intermolecular charge transfer in donor-acceptor substituted triarylmethane dye for NLO and optical limiting applications. *J. Mater. Sci. Mater. Elect.* 32: 9368–9376. <https://doi.org/10.1007/s10854-021-05600-7>.
9. Ryasnyansky AI, Palpant B, Debrus S, Khalibullin R, Stepanov RL (2006) Nonlinear optical properties of copper nanoparticles synthesized in indium tin oxide matrix by ion implantation. *J Opt Soc Am B* 23: 1348–1353. <https://doi.org/10.1364/JOSA.23.001348>.

10. Zeng H, Han J, Qian Q, Gu Y (2014) Third-order nonlinear optical properties of multiwalled carbon nanotubes modified by CdS nanoparticles. *Optik* 125: 6558–6531. <https://doi.org/10.1016/j.ijleo.2014.06.166>
11. Lee B, Kwon H, Kim S, Rotemund F (2016) Natural silk protein as a new broadband nonlinear optical materials. *Opt. Mater Express* 6: 993–1002. <https://doi.org/10.1364/OME.6.000993>.
12. Hernandez FZ, Marcano AO, Alvarado Y, Biondi A, Maillotte H (1998) Measurement of nonlinear refraction index and two-photon absorption in a novel organometallic compound. *Opt Commun* 152: 77–82. [https://doi.org/10.1016/S0030-4018\(98\)0053-9](https://doi.org/10.1016/S0030-4018(98)0053-9).
13. Kramer MA, Tompkin WR, Boyd RW (1986) Nonlinear optical interactions in fluorescein-doped boric acid glass. *Phys Rev A* 34: 2026–2031. <https://doi.org/10.1103/PhysRevA.34.2026>.
14. Bredas JL, Adant C, Tackx P, Persoons A, Pierce BM (1998) Third-order nonlinear optical response in organic materials: Theoretical and experimental aspects, *Chem Rev* 94: 243–278. <https://doi.org/10.1021/cr00025a008>.
15. Prasad PN, Williams DJ (1991) Introduction to nonlinear optical effects in molecules and polymers. Wiley New York.
16. Ch. Reichardt (1988) Solvent and Solvent Effects in Organic Chemistry, Wiley-VCH, Weinheim. Germany. 365–371.
17. Jeyaram S, Naseer J, Punitha S (2021) Effect of solvent on third-order nonlinear optical behavior of reactive blue 19 dye. *J Fluoresc* 31: 1895–1906. <https://doi.org/10.1007/s10895-021-02808-y>.
18. Jeyaram S (2021) Study of third-order nonlinear optical properties of basic violet 3 dye in polar protic and aprotic solvents. *J Fluoresc* 31: 1637–1644. <https://doi.org/10.1007/s10895-021-02796-z>.
19. Sheik-Bahae M, Said AA, Van Stryland EW (1989) High-sensitivity, single-beam  $n_2$  measurements. *Opt Lett* 14: 955–957. <https://doi.org/10.1364/OL.14.000955>.

20. Prakash A, Pathrose BP, Radhakrishnan P, Mujeep A (2020) Nonlinear optical properties of neutral red dye: Enhancement using laser ablated gold nanoparticles. *Opt Laser Technol* 130: 106338. <https://doi.org/10.1016/j.optlastec.2020.106338>.
21. Liu K, Sun D, Xu X, Shan W, Yao C, Sun W (2020) Ultrafast third-order nonlinear optical response of CdSe/Al<sub>2</sub>O<sub>3</sub>/Ag composite films. *Optik* 217: 164907. <https://doi.org/10.1016/j.ijleo.2020.164907>.
22. Kumar MK, Sudhakar S, Pandi P, Bhagavannarayana G, Kumar RM (2014) Studies of the structural and third-order nonlinear optical properties of solution grown 4-hydroxy-3-methoxy-4'-N'-methylstilbazolium tosylate monohydrate crystals. *Opt Mater* 36: 988–995. <https://doi.org/10.1016/j.optmat.2014.01.007>.
23. Mgidlana S, Sen P, Nyokong T (2020) Direct nonlinear optical absorption measurements of asymmetrical zinc (II) phthalocyanine when covalently linked to semiconductor quantum dots. *J Mol Struct* 1220: 128729. <https://doi.org/10.1016/j.molstruc.2020.128729>.

**Table 1** TNLO properties of QCC in polar solvents

Solvents	$n_2 \times 10^{-11}$ (m <sup>2</sup> /W)	$\beta \times 10^{-5}$ (m/W)	$\text{Re}(\chi^{(3)}) \times 10^{-7}$ (esu)	$\text{Im}(\chi^{(3)}) \times 10^{-7}$ (esu)	$\chi^{(3)} \times 10^{-7}$ (esu)
DMSO	-2.35	6.61	-9.47	1.37	9.50
DMF	-1.06	6.38	-3.96	1.23	4.15
Ethanol	-0.68	-6.56	-2.30	-1.15	2.57

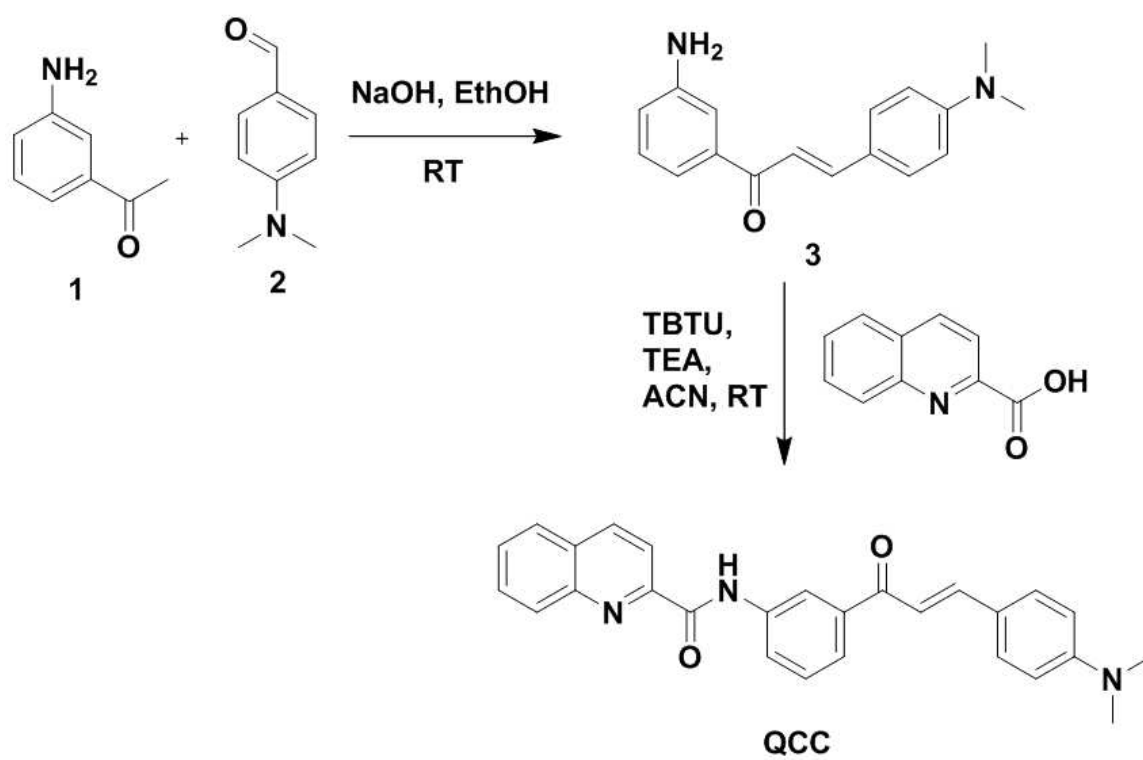


Fig.1 Synthesis procedure of QCC

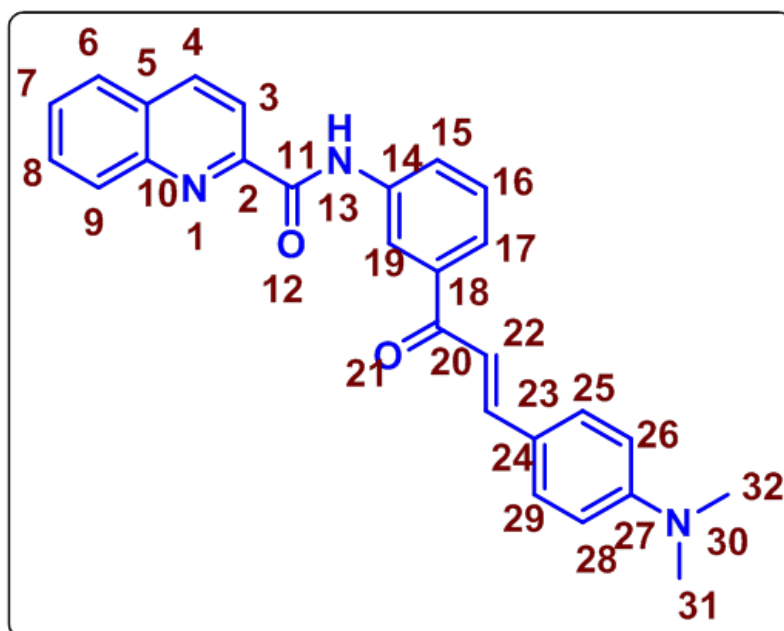


Fig. 2 Molecular structure of QCC

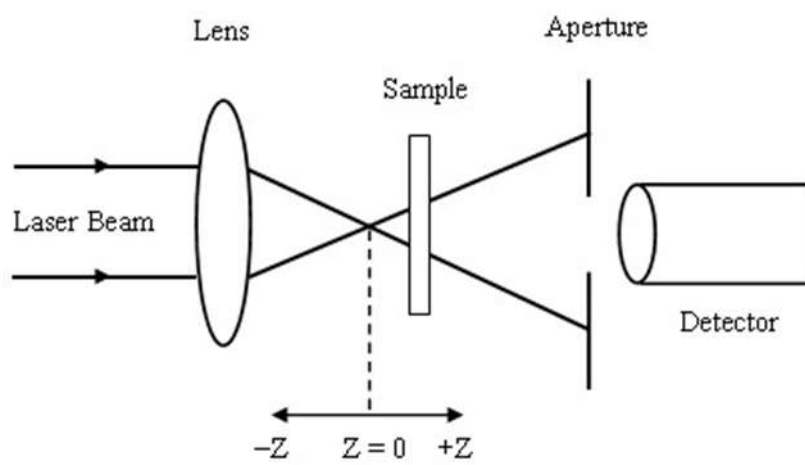
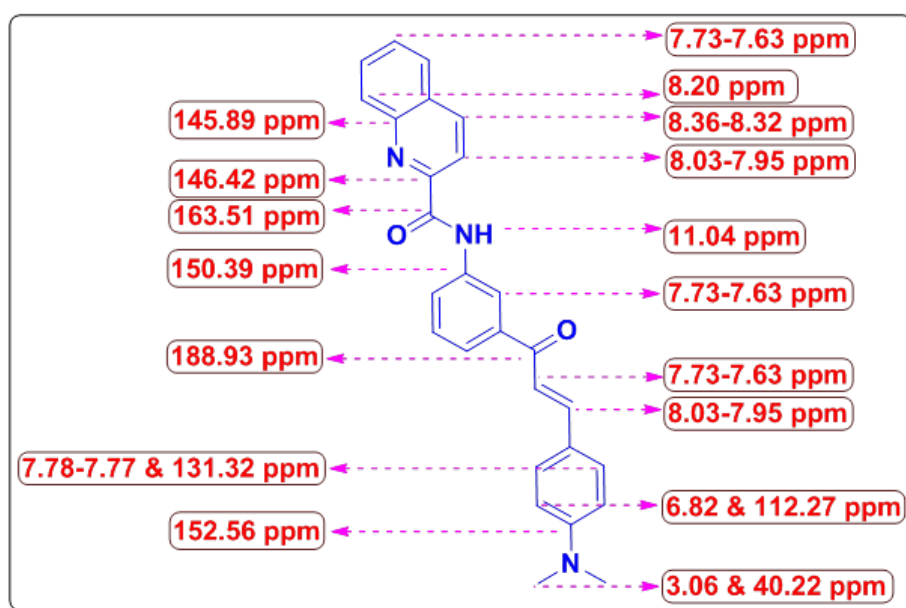


Fig.3 Experimental arrangement of Z-scan technique



F

ig. 4 Selected <sup>1</sup>H NMR <sup>13</sup>C NMR chemical shifts of QCC

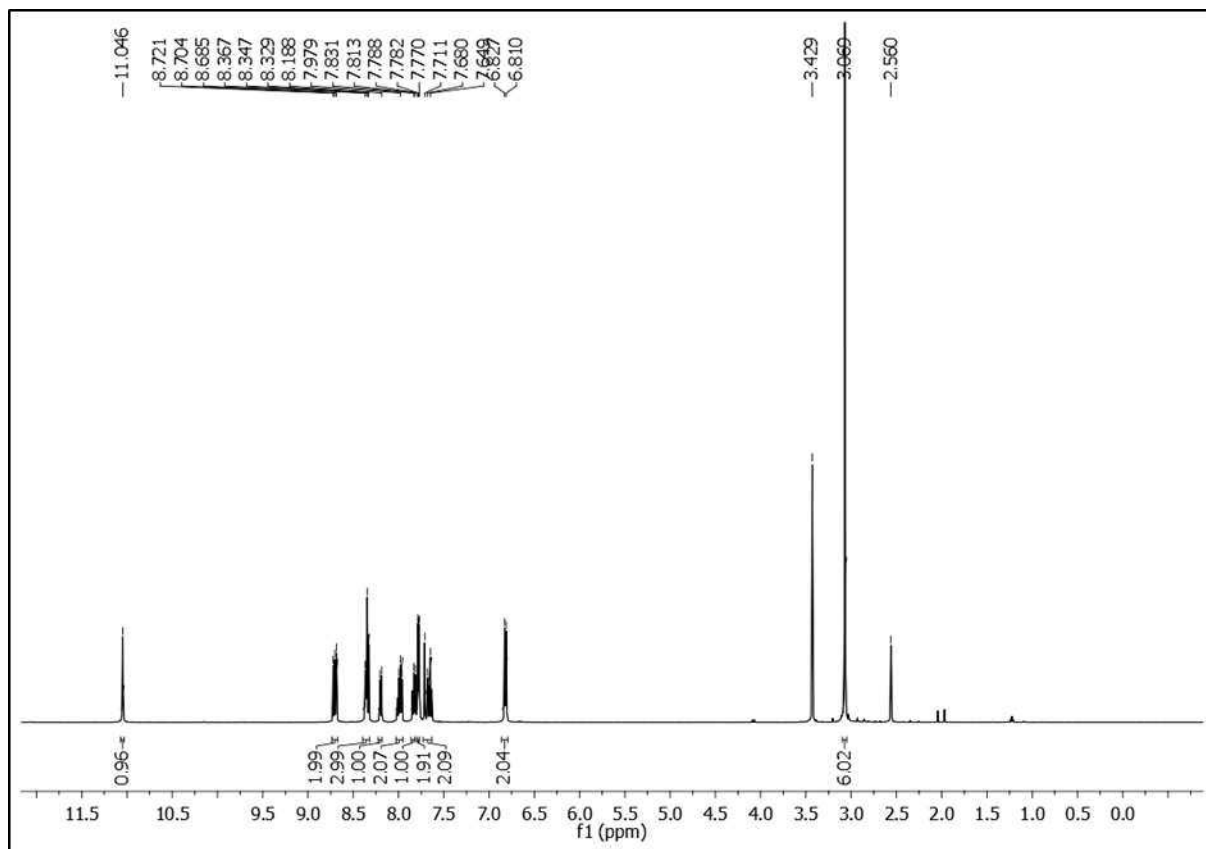


Fig. 5 <sup>1</sup>H NMR spectrum of QCC

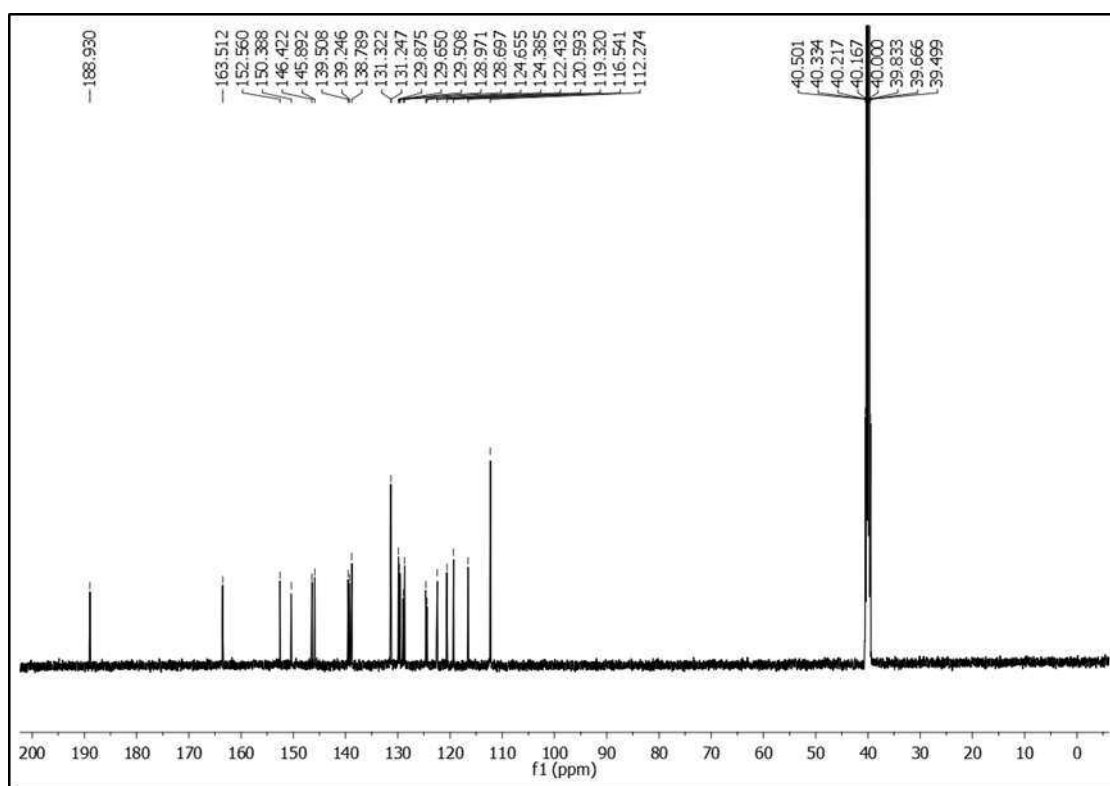


Fig. 6  $^{13}\text{C}$  NMR spectrum of QCC

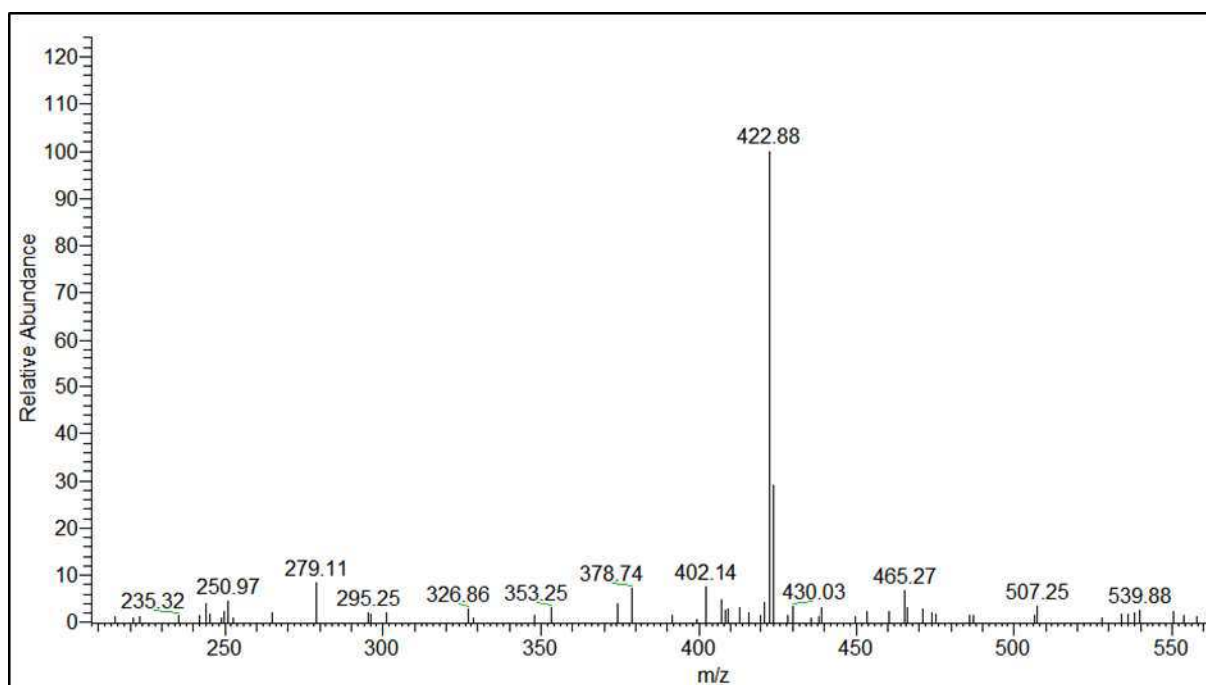


Fig. 7 ESI-Mass spectrum of QCC

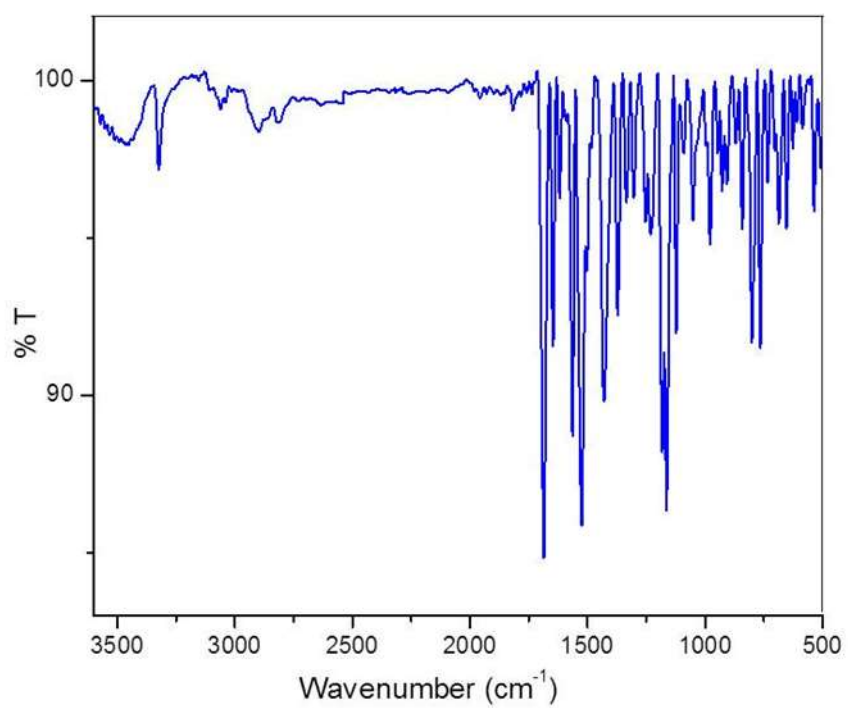


Fig. 8 FT-IR spectra of QCC

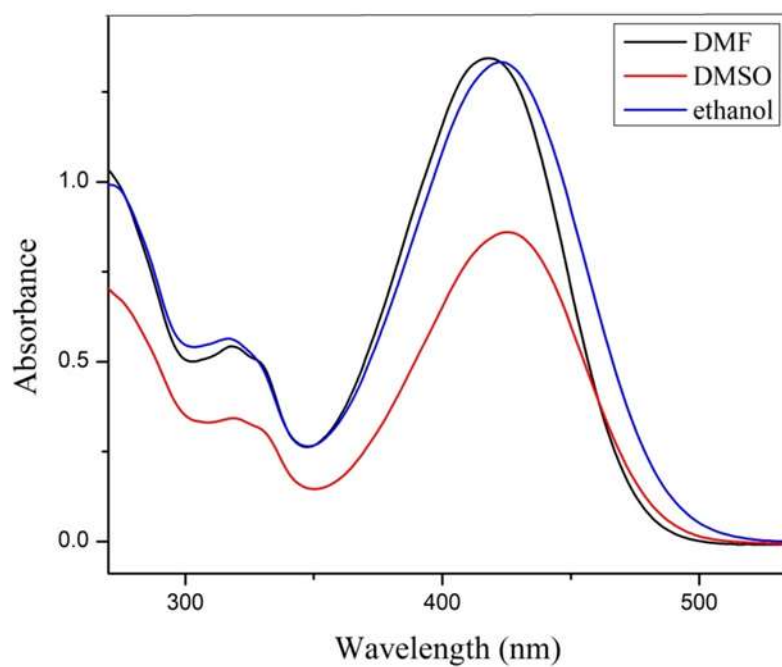


Fig. 9 UV-Visible absorption spectra of QCC dissolved in polar solvents

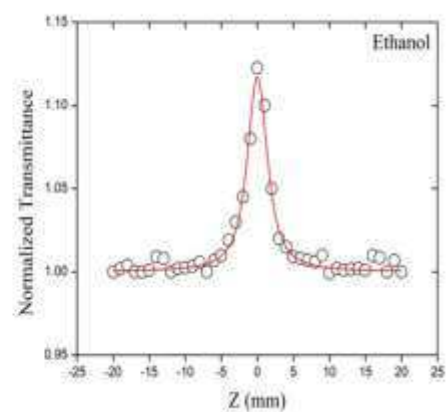
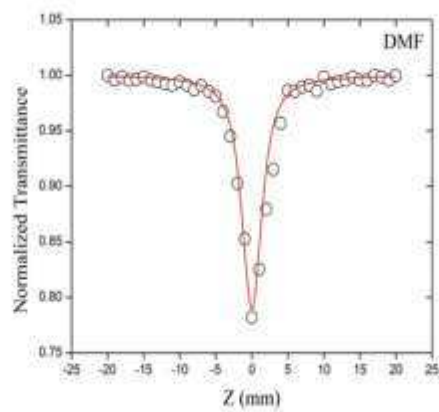
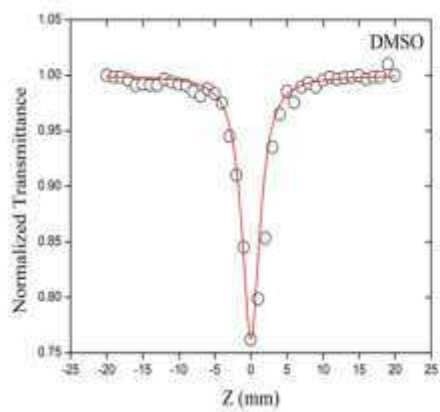


Fig.10 OA normalization curve of QCC dissolved in different polar solvents

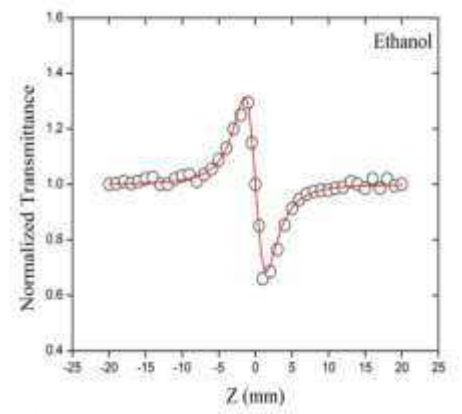
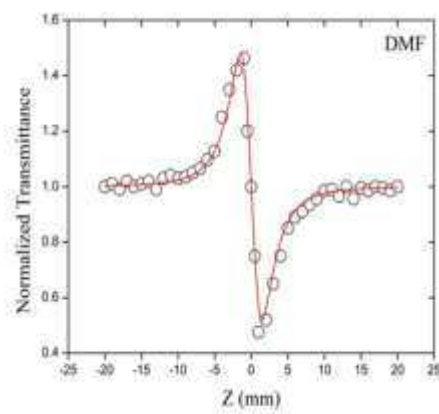
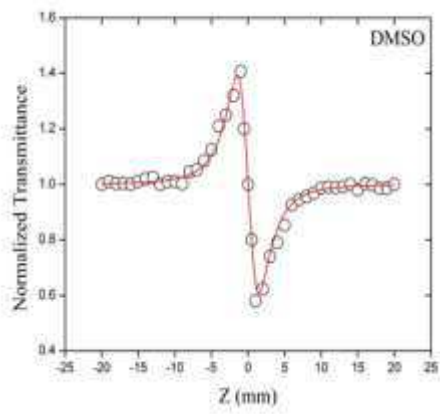


Fig.11 CA normalization curve of QCC dissolved in different polar solvents

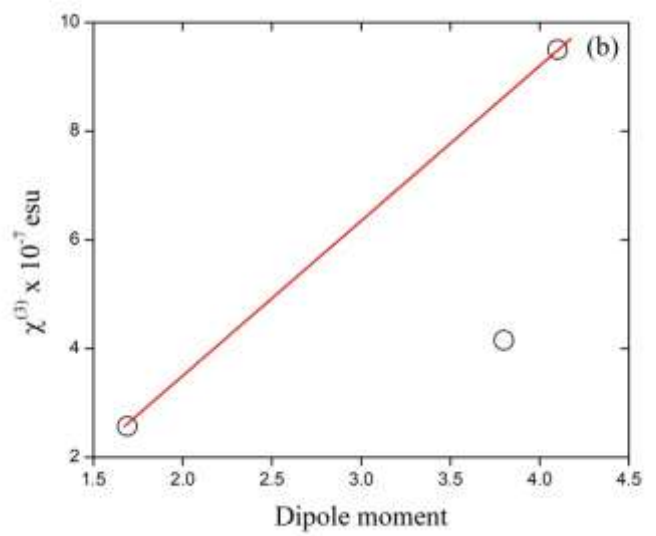
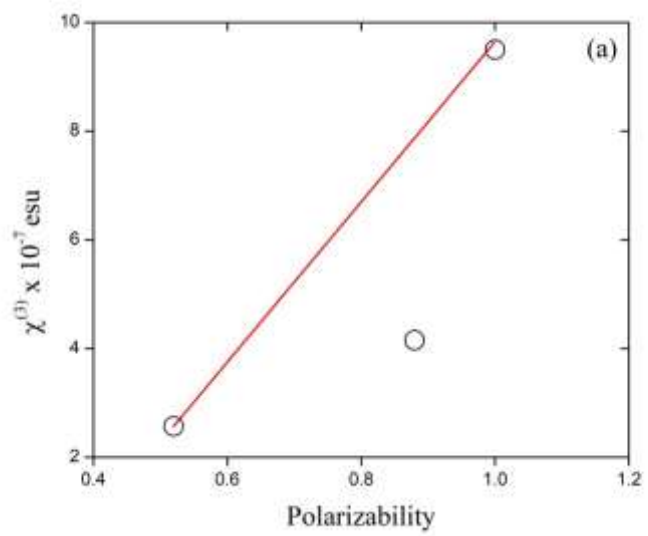


Fig. 12 Variation of TNLO susceptibility of QCC as a function of (a) Polarizability (b) dipole moment